Veröffentlichung

Autoren

Rurkowska, Katherina;Langer, Sabine

Titel

Coupling elastic-poroelastic material in structure-borne sound modelling

Publisher o. Konferenz

Acoustical Society of America, Proceedings of Meetings on Acoustics, Vol. 19, 030073 (2013)

Jahr

2013

Internet-Link (Doi-Nr.)

Proceedings of Meetings on Acoustics

Volume 19, 2013 http://acousticalsociety.org/

ICA 2013 Montreal
Montreal, Canada
2 - 7 June 2013

Engineering Acoustics
Session 3pEA: Computational Methods in Transducer Design, Modeling, Simulation, and Optimization III

3pEA1. Coupling elastic-poroelastic material in structure-borne sound modelling

Katherina Rurkowska* and Sabine Langer

***Corresponding author's address: Institut für Angewandte Mechanik, Technische Universität Braunschweig, Spielmannstraße 11, Braunschweig, 38106, Niedersachsen, Germany, k.rurkowska@tu-braunschweig.de**

Porous materials are widely used in noise reduction applications. To minimize the external noise produced by aicraft propeller drives, porous materials are implemented. As a part of the project Sonderforschungsbereich 880 "Fundamentals of High Lift for Future Civil Aircraft", porous surfaces are used in the High-lift configuration to mitigate the flow noise and to influence the structure-borne sound. In order to model the performance of the applied poroelastic material, an approach coupling a poroelastic material with an elastic structure using Finite Element Method is presented. The Biot's theory is used to model the poroelastic material. The aim of this work is to simulate the effect of the entry and transmission of the structure-borne sound into the poroelastic medium. An example of the implemented model shows the plausibility of presented approach.

Published by the Acoustical Society of America through the American Institute of Physics

 [DOI: 10.1121/1.4796035]
Received 22 Jan 2013; published 2 Jun 2013

INTRODUCTION

Porous surfaces are studied for application in high-lift configuration of aircrafts to mitigate the flow noise and to influence the structure-borne sound [1]. The goal is the accurate modeling and calculation of the entry and the transmission of structure-borne sound which results from flow fields. These studies provide a necessary basis to allow an evaluation of the new configuration in reference to cabin noise. The current work focuses on the modeling of the interaction between an elastic structure and porous materials in order to simulate the effect of porous surfaces on structure-borne sound. The modeling of flow-induced vibrations of poroelastic materials is presented in [2] [3] and thoroughly detailed in [4]. Porous materials can be described with different detailed models: impedance models, equivalent fluid approaches and poroelastic models [5]. To describe the properties of poroelastic materials, there are two formulations: the Biot's theory, and the theory of porous media (TPM). In the Biot's formulation, the behavior of the two phases of the porous medium is described by their fluid-structure interaction. To describe the behaviour of the porous materials, a displacement-pressure (u,p) formulation based on Biot is used here [6, 7]. The numerical simulation is carried out using the Finite Element Method (FEM) implemented in the in-house code *elPaSo*.

MODELING AND SIMULATION

Porous Material

Porous materials consist of two phases: a solid phase and fluid-filled pores. The (u,p) equation of motion for the solid phase of the poroelastic material is given by

$$\hat{\sigma}^s_{ij,j} + \tilde{\varrho}\omega^2 u^s_i + \tilde{\gamma} p_{,i} = 0 \tag{1}$$

where

$$\tilde{\varrho} = \tilde{\varrho}_{11} - \frac{(\tilde{\varrho}_{12})^2}{\tilde{\varrho}_{22}} \tag{2}$$

and

$$\tilde{\gamma} = \phi\left(\frac{\tilde{\varrho}_{12}}{\tilde{\varrho}_{22}} - \frac{\tilde{Q}}{\tilde{R}}\right). \tag{3}$$

$\hat{\sigma}^s_{ij}$ denotes the stress tensor of the solid phase. The indeces s and f correspond to the solid and fluid phase, respectively. The equation of motion for the fluid phase is given by

$$\sigma^f_{ij} = -\phi p^f \delta_{ij} = \tilde{R} u^f_{k,k}\delta_{ij} + \tilde{Q} u^s_{k,k}\delta_{ij}. \tag{4}$$

Eq.(5) gives the (u,p) formulation.

$$p_{,ii} + \frac{\tilde{\varrho}_{22}}{\tilde{R}}\omega^2 p - \frac{\tilde{\varrho}_{22}}{\phi^2}\tilde{\gamma}\omega^2 u^s_{i,i} = 0. \tag{5}$$

ϕ denotes porosity and $\tilde{\varrho}$, $\tilde{\gamma}$, $\tilde{\varrho}_{12}$, $\tilde{\varrho}_{22}$, $\tilde{Q}$, $\tilde{R}$ are Biot's formulation parameters [8].

Structure

The structure is described as a shell using the Mindlin plate theory for plate of moderate thickness $(h/\ell < 0,2)$ in combination with a disc formulation. Equation (6) presents the equation of motion according to Mindlin

$$B\Delta\Delta\hat{u}_z + \omega^2\varrho\left(\frac{B}{Gk_s} - I\right)\Delta\hat{u}_z - \omega^2\varrho h\hat{u}_z + \omega^4\varrho\frac{I}{Gk_s}\hat{u}_z = \hat{p}_z - \frac{B}{Ghk_s}\Delta\hat{p}_z - \omega^2\varrho\frac{I}{Ghk_s}\hat{p}_z. \tag{6}$$

where B is the flexural stiffness $EI/1-\nu^2$. G denotes the shear modulus $E/(2(1+\nu))$, E is Young's modulus und ϱ the density, I the moment of inertia and ν the Poisson's ratio. k_S presents the shear correction factor and is assumed to be $k_s = 5/(6-\nu)$ and h is the plate's thickness. u represents displacement, and p stands for pressures acting on the plate. Δ is the Laplace-Operator $\frac{\partial^2}{\partial x^2} + \frac{\partial^2}{\partial y^2}$ and ω the angular frequency. Detailed derivations of the differential equations for plate vibrations are found in [9, 10, 11, 12].

Interaction of poroelastic material and structure

At the interface between the structure and the porous material, the following conditions must be fulfilled [13]:

$$\begin{aligned}(\sigma_{ij}^t)^p \cdot n_j &= (\sigma_{ij}^t)^{str} \cdot n_j,\\ u_i^s &= u_i^{str},\\ \left(u_i^f - u_i^s\right) n_i &= 0.\end{aligned} \tag{7}$$

The index p denotes the poroelastic material and str the elastic structure and f and s the fluid and solid phases of the porous material, respectively. The first coupling condition ensures the continuity of the stresses at the interface, and the second indicates that the solid phase of the porous material and the elastic structure are connected and undergo the same deflections. The third condition relates the velocity of the solid and fluid phase in the normal direction, so that there is no mass flow across the interface. To implement this coupling conditions into the FE formulation, I_1 and I_2 must be considered as boundary loads on the solid or fluid phase. The approximation of the displacements u and the pressure p by shape functions N and the choice of weight functions according to the Galerkin method, leads to the following contributions per interface:

$$I_1 = -\vec{c}^{pstr}\vec{p} = -\phi\left(1+\frac{\tilde{Q}}{\tilde{R}}\right)\int_A (\vec{N}^s)^T \vec{n}\vec{N}^f \, dA\,\vec{p}, \tag{8}$$

$$I_2 = -\omega^2(\vec{c}^{pstr})^T\vec{u} = -\omega^2\phi\left(1+\frac{\tilde{Q}}{\tilde{R}}\right)\int_A (\vec{N}^f)^T \vec{n}^T\vec{N}^s \, dA\,\vec{u}. \tag{9}$$

Assuming no external forces acting on the interface, a Finite Element system of equations for the nodes at the coupling surface is obtained. It includes the matrix contributions of the porous material $\vec{K}^{ss}$, $\vec{M}^{ss}$, $\vec{C}^{sf}$, $\vec{K}^{ff}$ and $\vec{M}^{ff}$ and the stiffness matrix $\vec{K}^{str}$ and the mass matrix $\vec{M}^{str}$ of the shell elements of the structure.

$$\begin{bmatrix} (\vec{K}^{ß}+\vec{K}^{str}) - \omega^2(\vec{M}^{ss}+\vec{M}^{str}) & -\vec{C}^{sf} - \vec{C}^{pstr} \\ -\omega^2((\vec{C}^{sf})^T + (\vec{C}^{pstr})^T) & \vec{K}^{ff} - \omega^2\vec{M}^{ff} \end{bmatrix} \begin{bmatrix}\vec{u}\\ \vec{p}\end{bmatrix} = \begin{bmatrix}\vec{0}\\ \vec{0}\end{bmatrix} \tag{10}$$

Numerical Example

As verification example, a rectangular shell plate with simply supported edges is studied. A comparison with results by Debergue *et al.* is carried out [14]. The plate is connected to a poroelastic layer and excited by a plane wave with the amplitude of P = 0.02 Pa (see figure 1). The details of the geometry and

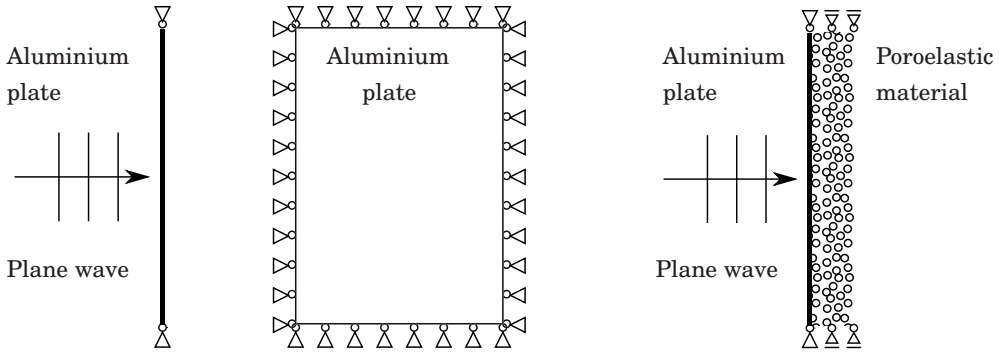

(A) Simply supported aluminium plate

(B) Simply supported aluminium plate with porous material layer

Figure 1: Numerical example setting

material properties are listed in tables 1. At the edges, the poroelastic material is simply supported, in addition displacements perpendicular to the plate are allowed. Two cases with different conditions at the

TABLE 1: Material parameters

(A) Aluminium plate

Thickness	$d = 0.001$ m
Lenght	$a = 0.35$ m
Width	$b = 0.22$ m
Density	$\varrho = 2742$ kg/m^3
Young's modulus	$E = 6.9 \cdot 10^{10}$ N/m^2
Poisson's ratio	$\nu = 0.33$
Loss factor	$\eta = 0.007$

(B) Porous material (foam)

Thickness	$d = 0.05$ m
Flow resistance	$\sigma = 13500$ Ns/m^4
Porosity	$\phi = 0.98$
Tortuosity	$\alpha_\infty = 1.7$
Viscous characteristic length	$\Lambda = 80 \cdot 10^{-6}$ m
Thermal characteristic length	$\Lambda' = 160 \cdot 10^{-6}$ m
Density solid phase	$\varrho_1 = 30$ kg/m^3
Young's modulus solid phase	$E = 5.4 \cdot 10^5$ N/m^2
Poisson's ratio	$\nu = 0.35$
Loss factor	$\eta = 0.1$

open surface of the poroelastic material are carried out: 1. *in vacuo* conditions (modelled by a Dirichlet condition set to zero) and 2. impedance conditions ($Z_0 = 415 Ns/m^3$).

The aluminium plate is discretized using two-dimensional shell elements, and the porous material using three-dimensional elements. Both types of elements use quadratic shape functions. The mesh consists of 23 x 17 elements and 4 elements in the direction of the thickness of the porous materials. The simulation is carried out using the Finite Element Method implemented in the in-house code *elPaSo*. The FEM calculation is performed for the frequency range from 10 to 500 Hz. For each frequency, the deflection of the disk is determined as the mean square displacement and converted to the velocity. The representation in decibel [dB] is given by the usual conversion formula, based on the ratio of a value of variable X and reference variable X_0 , namely $v_0 = 5 \cdot 10^{-8} m/s$ for the velocity.

$$X\ [\text{dB}]\ = 10 \log \left(\frac{X}{X_0} \right)^2 = 20 \log \frac{X}{X_0} \tag{11}$$

Figure 2 presents the comparison of the results according to Debergue *et al.* and the results carried out using the in-house code *elPaSo*. In general, the results show good agreement. The location and the

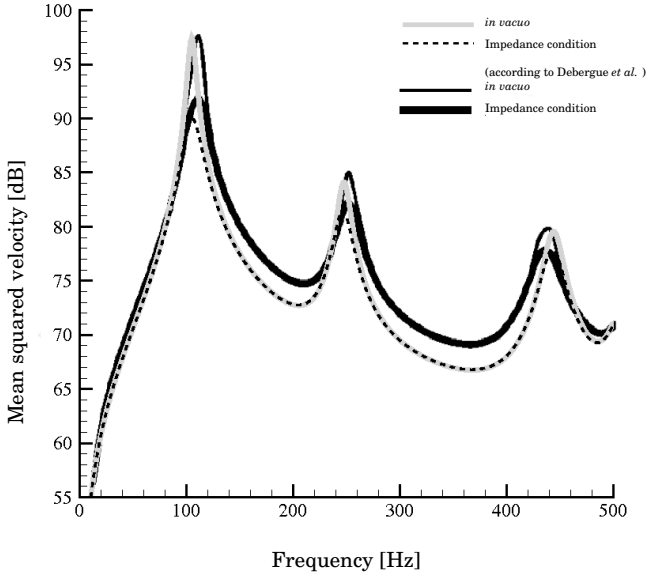

FIGURE 2: Results carried out using the in-house code *elPaSo* compared with Debergue *et al.* [14]

values of the eigenfrequencies are in good agreement, up to the first eigenfrequencies. The discrepancies in the higher frequency range can be explained by the discretization, that satisfy the criterion of six nodes per wavelength only up to 300 Hz. For the existing discrepancies between the peaks no obvious explanation can be given. It has to be studied if the differing results are due to minor differences in the

TABLE 2: Porous material parameters taken from literatur

	mineral wool [5]	felt [15]
Flow resistance	$\sigma = 40000$ Ns/m^4	$\sigma = 33000$ Ns/m^4
Porosity	$\phi = 0.94$	$\phi = 0.98$
Tortuosity	$\alpha_\infty = 1.6$	$\alpha_\infty = 1.1$
Viscous characteristic length	$\Lambda = 56 \cdot 10^{-6}$ m	$\Lambda = 50 \cdot 10^{-6}$ m
Thermal characteristic length	$\Lambda' = 110 \cdot 10^{-6}$ m	$\Lambda' = 110 \cdot 10^{-6}$ m
Density solid phase	$\rho_1 = 130$ kg/m^3	$\rho_1 = 60$ kg/m^3
Young's modulus solid phase	$E = 4.4 \cdot 10^6$ N/m^2	$E = 1.0 \cdot 10^5$ N/m^2
Poisson's ratio	$\nu = 0$	$\nu = 0$
Loss factor	$\eta = 0.1$	$\eta = 0.88$

implementation of the numerical elements that show up in the vibrational behavior when excited out of the eigenfrequencies. Furthermore, only the results *in vacuo* cases are considered. Figure 3 compares the vibrational behaviour of the plate with and without a porous layer. A general reduction of the vibration

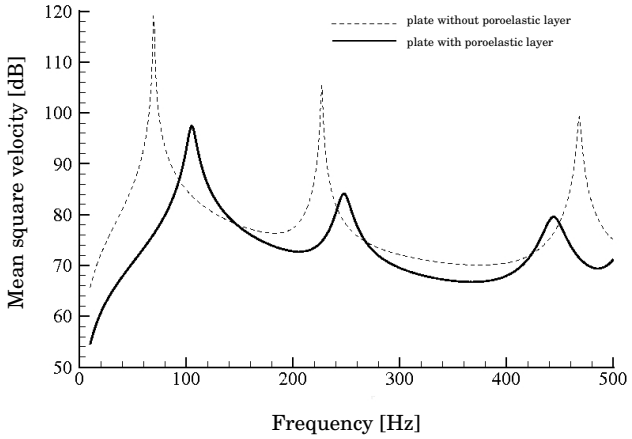

FIGURE 3: Mean square velocity with and without porous material

velocities can be observed. In particular, the velocity peaks on the eigenfrequency of the plate are damped. In the whole range of frequencies, a shift of the position of the eigenfrequencies is observed as well. A poroelastic layer does not increase exclusively the structural damping, but rather means a change in the overall structural behavior. The structural behaviour depends on the properties of the porous materials. Figure 4 presents the comparison of the aluminium plate combined with the above specified foam, with mineral wool or with felt. The material data are taken from the literature and listed in table 2.

The combination of the plate with mineral wool with a high Young's modulus ($E = 4.4 \cdot 10^6$ N/m^2) results in a stiffer system, compared to the combination with the foam ($E = 5.4 \cdot 10^5$ N/m^2). It can be observed in figure 4 that the first eigenfrequency of the plate-mineral wool system is shifted to a higher frequency. Whereas in to the combination with felt, the first eigenfrequency is shifted to a lower frequency as a result of a softer system. The results of the plate/felt combination show, after the first eigenfrequency, a curve with only a recognizable first eigenfrequency due to a high loss factor $\eta = 0.88$ in comparison with the other porous materials.

OUTLOOK

A model for coupling elastic and porous material has been presented and validated. The presented studies illustrate the effect of porous layers on structural vibrations. The implemented numerical method enables the determination of the effect of porous layer on sound radiation and sound transmission. Studies on applications in high-lift configurations will be held combining the presented approach with the model for flow-induced sound in poroelastic materials presented in [4].

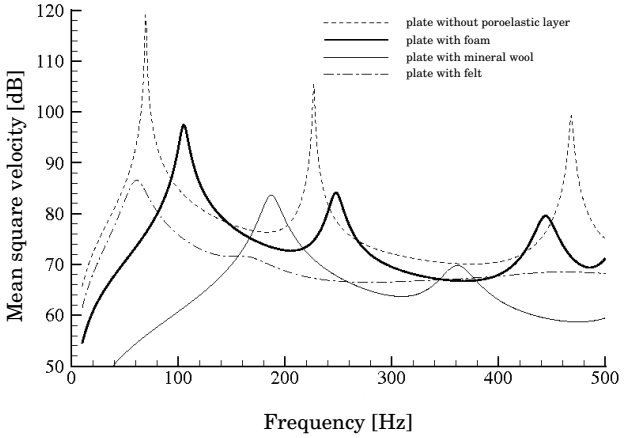

FIGURE 4: Mean square velocities for the combination with different porous materials

ACKNOWLEDGMENTS

The authors would like to thank the *Sonderforschungsbereich 880 of the Deutsche Forschungsgemeinschaft* and its graduate reseach program *Modul Graduiertenkolleg (MGK)* for the financial support.

REFERENCES

[1] "Biennal Report 2012/13, Collaborative Research Center 880 (CRC)", Campus Forschungsflughafen Braunschweig (2013), to appear.

[2] S. Beck and S. Langer, "Modellierung von strömungsinduzierter Schalleinleitung in poroelastische Materialien", in *Proceedings of DAGA 2012*, 927–928 (2012).

[3] S. C. Beck, *Strömungsinduzierter Körperschalleintrag in Strukturen mit porösen Oberflächen*, volume 66 (Braunschweiger Schriften zur Mechanik) (2012).

[4] M. Zahid, S. Langer, and S. Beck, "Modeling of flow-induced sound in poroelastic materials", in *Proc. of 5th BIOT Conference on Poromechanics (BIOT-5)* (2013), to appear.

[5] J. F. Allard and N. Atalla, *Propagation of Sound in Porous Media* (John Wiley & Sons, Ltd.) (2009).

[6] M. A. Biot, "Theory of propagation of elastic waves in a fluid-saturated porous solid. i. low-frequency range", Journal of the Acoustical Society of America **28**, 168–178 (1956).

[7] M. A. Biot, "Theory of propagation of elastic waves in a fluid-saturated porous solid. ii. higher frequency range", Journal of the Acoustical Society of America **28**, 179–191 (1956).

[8] N. Atalla, R. Panneton, and P. Debergue, "A Mixed Displacement-Pressure Formulation for Poroelastic Materials", Journal of the Acoustical Society of America **104**, 1444–1452 (1998).

[9] L. Cremer and M. Heckl, *Körperschall* (Springer, Berlin, Heidelberg) (1996).

[10] L. Ackermann, *Simulation der Schalltransmission durch Wände*, volume 43 (Braunschweiger Schriften zur Mechanik) (2002).

[11] D. Clasen, *Numerische Untersuchung der akustischen Eingenschaften von trennenden und flankierenden Bauteilen*, volume 64 (Braunschweiger Schriften zur Mechanik) (2008).

[12] D. Clasen and S. Langer, "Consideration of flanking transmission within numerical simulation of sound insulation", in *Proc. EuroNoise 2006* (2006).

[13] R. Panneton and N. Atalla, "Numerical prediction of sound transmission through finite multilayer systems with poroelastic materials", Journal of the Acoustical Society of America **100**, 346–354 (1996).

[14] P. Debergue, R. Panneton, and N. Atalla, “Boundary Conditions for the Weak Formulation of the Mixed (u,p) Poroelasticity Problem”, Journal of the Acoustical Society of America **106**, 2383–2390 (1999).

[15] C. Batifol, T. G. Zielinski, M.-A. Galland, and M. N. Ichchou, “Hybrid piezo-poroelastic sound package concept: Numerical/experimental validations”, in *Proceedings of Active 2006* (Sixth International Symposium on Active Noise and Vibration Control, Adelaide, Australia) (2006).